# Longitudinal recoil-ion momentum distribution in ionization collisions by neutral projectiles near the kinematical threshold

V. D. Rodríguez
*Departamento de Física, Facultad de Ciencias Exactas y Naturales, Universidad de Buenos Aires, 1428 Buenos Aires, Argentina*

R. O. Barrachina
*Comisión Nacional de Energía Atómica, Centro Atómico Bariloche e Instituto Balseiro, 8400 Bariloche, Argentina*
(Received 13 September 1995)

In a previous paper it has been shown that the longitudinal recoil-ion momentum (RIM) distribution for the single ionization of atoms by charged ions exhibits a finite value at the kinematic threshold. This structure can be ascribed to the divergence of the electron capture to the continuum peak in the ionization cross section. We generalize this result for the case of a neutral projectile. In particular we show that a sharp peak of the RIM distribution at the threshold can occur for given final-state electron-projectile systems. [S1050-2947(96)04905-0]

PACS number(s): 34.10.+x, 34.50.Fa

## I. INTRODUCTION

The velocity distribution of electrons emitted from an atomic target by the collision of an energetic ion has been actively investigated during the past three decades (see, for instance [1]). This sustained interest has been prompted by the information that it provides about the interactions and mechanisms involved in the ionization process. From previous work the electron spectrum has been characterized according to the momentum space regions of the emitted electrons. For illustration we show in Fig. 1 the ionization cross section $d\sigma/d^3\mathbf{k}_e$ for a $H^+ + He$ collision at 625 keV (projectile velocity $v=5$ a.u.). Three conspicuous features of this distribution are the binary encounter sphere [2] and two cusp-shaped peaks centered in momentum space about the origin [''soft electrons (SE)''] [3] and $m\mathbf{v}$ [''electron capture to the continuum (ECC)''] [4–6], where $m$ is the mass of the electron and $\mathbf{v}$ is the velocity of the incident projectile. The first process occurs when an electron initially bound to the target atom is expelled by an elastic binary encounter with the projectile, giving rise to a shoulder in the momentum distribution located on a ''sphere'' of a radius approximately equal to $mv$ and centered about $\mathbf{k}_e = m\mathbf{v}$. The momentum distribution of this bound state determines the shape of the shoulder in the ionization cross section $d\sigma/d^3\mathbf{k}_e$. On the other hand, the SE and ECC peaks have been traditionally attributed to a mechanism where the ejected electron ends up in a low-lying continuum state of the ''charged'' residual target or projectile.

Let us now concentrate on this ECC effect. We can observe in Fig. 1 the known cusp shape of the ECC peak. The precise measurement of this peak has been an elusive task due to the extreme sensitivity of its shape on the angular and energy resolution of the electron analyzer [7,8]. In particular, a precise determination of the shape at the very top of the peak remains as an unsolved problem.

Quite recently, improvements [9,10] in the technique of cold-target recoil-ion momentum spectroscopy have provided an indirect way of performing such a measurement. Actually, it has been shown that the divergence of the ECC peak in the single ionization cross section for ion-atom collisions is related to a finite value of the longitudinal recoil-ion momentum (RIM) distribution at the kinematic threshold [11]. In this paper we generalize this result for nonbare ion impact, showing how the behavior of the longitudinal RIM distribution at the kinematic threshold represents a distinctive fingerprint of the ECC peak structure. In particular we show that this distribution can display a sharp peak or even a divergence at the threshold that can be ascribed to certain features of the electron-projectile system in the final state.

The paper is organized as follows. Section II summarizes the theory based on the final-state interaction theory [12,13]. Then the ionic projectile case is presented in Sec. III. Section IV presents the case of neutral projectiles for three different electron-projectile final-state interactions. Final remarks are given in Sec. V.

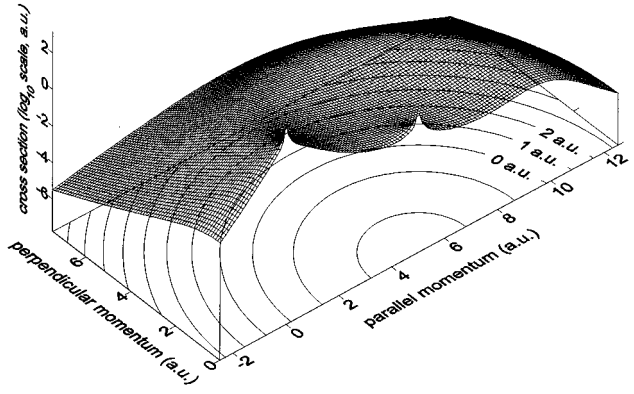


FIG. 1. Ionization cross section $d\sigma/d^3\mathbf{k}_e$ for a $H^+ + He \rightarrow H^+ + He^+ + e^-$ collision at 625 keV ($v=5$ a.u.). The lines of constant longitudinal recoil-ion momentum $P_{R\|}$ are shown as ''circles'' on the electron momentum ''plane'' centered about the ECC peak. In particular, the binary electrons can be identified as those located at the $P_{R\|}=0$ circle.

 © 1996 The American Physical Society

## II. THEORY

According to the final-state interaction theory [12,13], the behavior of the ionization cross section for small values of the relative electron-projectile momentum $\mathbf{p}=\mathbf{k}_e-m\mathbf{v}$ can be shown to be dominated by the normalization of the corresponding continuum wave function $\Psi_p(\mathbf{r}')$ for the electron-projectile system [14,15]. This defines a normalization factor (atomic units are used throughout)

$$F(p)=(2\pi)^3|\Psi_p(0)|^2. \tag{1}$$

The general properties of this factor can be identified easily, even without a complete knowledge of the actual electron-projectile interaction. First, it is greater (lower) than one for any generally attractive (repulsive) potential, and therefore the actual effect of the distortion is to enhance (decrease) the cross section. Second, since $|\Psi_p(0)|^2\rightarrow(2\pi)^{-3}$ for large $p$, this normalization factor is dominant for small electron-projectile velocities. In particular, for an ionic projectile of charge $Z_P$ the normalization factor can be easily evaluated as

$$F(p)=\frac{2\pi Z_P/p}{1-\exp(-2\pi Z_P/p)}. \tag{2}$$

For small values of $p$ this factor approaches zero exponentially when $Z_P<0$,

$$F(p)\approx\frac{2\pi|Z_P|}{p}\exp(-2\pi|Z_P|/p), \tag{3}$$

and diverges when $Z_P>0$ as

$$F(p)\approx\frac{2\pi Z_P}{p}. \tag{4}$$

After integrating over the spectrometer resolution, this latter behavior leads to the known cusp shape of the ECC peak, as shown in Fig. 1.

Let us now show how the relation between the longitudinal RIM distribution at the threshold and the ECC peak arises. Basically, it emerges as an offspring of the dynamic constraints required by energy and momentum conservation. In the longitudinal direction we obtain after some simple algebra a one-to-one relation between the longitudinal momentum $P_{R\|}$ of the recoil ion in the laboratory frame and the modulus of the relative electron-projectile momentum $\mathbf{p}$,

$$P_{R\|}=-\frac{v}{2}+\frac{|\varepsilon_i|}{v}+\frac{p^2}{2v}, \tag{5}$$

where $\varepsilon_i$ is the binding energy of the initial target electron. In this equation we have neglected terms of order $1/M_P$ and $1/M_T$, where $M_P$ and $M_T$ are the masses of the projectile and target, respectively.

We clearly see that there exists a threshold in the longitudinal recoil-ion momentum given by

$$P_{R\|}^{\min}=-\frac{v}{2}+\frac{|\varepsilon_i|}{v}, \tag{6}$$

which corresponds to $p=0$ ($\mathbf{k}_e=\mathbf{v}$), that is, to the ECC peak in the electron momentum distribution. On the other hand, Eq. (5) relates each particular value of $P_{R\|}$ to a ''sphere'' on the electron momentum space with radius $\sqrt{2v(P_{R\|}-P_{R\|}^{\min})}$ and centered about the ECC peak, as is shown in Fig. 1. In particular, the binary electrons can be identified as those located at the $P_{R\|}=0$ sphere [11]. On the other hand, soft-electron emission ($\mathbf{k}_e\sim\mathbf{0}$) is associated with $P_{R\|}^{s}=|\varepsilon_i|/v$, as can be obtained from Eq. (5).

Generally, for any given value of $P_{R\|}$, the longitudinal RIM distribution can be obtained by integrating the ionization cross section over the corresponding sphere in the electron momentum space

$$\frac{d\sigma}{dP_{R\|}}=\int\frac{d\sigma}{d\mathbf{k}_e}\,\delta(P_{R\|}-P_{R\|}^{\min}-p^2/2v)\,d^3\mathbf{k}_e. \tag{7}$$

Changing variables from $\mathbf{k}_e$ to $\mathbf{p}$ by a simple Galilean transformation, it can be shown easily that $d\sigma/dP_{R\|}$ is simply related to the ionization cross section differential in the modulus of the electron-projectile relative momentum

$$\frac{d\sigma}{dP_{R\|}}=\frac{v}{p}\frac{d\sigma}{dp} \tag{8}$$

with

$$p=\sqrt{2v(P_{R\|}-P_{R\|}^{\min})} \tag{9}$$

and

$$\frac{d\sigma}{dp}=p^2\int\frac{d\sigma}{d\mathbf{k}_e}\,d\hat{\mathbf{p}}. \tag{10}$$

It is interesting that for the longitudinal transferred momentum $\mathbf{P}_{P\|}=(\mathbf{K}_f-\mathbf{K}_i)\cdot\hat{\mathbf{v}}$ formulas (6)–(9) hold if we replace $\mathbf{p}$ by $\mathbf{k}_e$ and $\mathbf{P}_{R\|}$ by $\mathbf{P}_{P\|}$. Thus there is a symmetry: (recoil target, momentum $\mathbf{p}$)$\leftrightarrow$(projectile, momentum $\mathbf{k}_e$).

Let us study the RIM cross section $d\sigma/dP_{R\|}$ near the kinematical threshold, that is, for $p\rightarrow0$. As we are near the ECC peak, we adopt the conventional parametrization [16]

$$\frac{d\sigma}{d^3\mathbf{k}_e}=F(p)\sum_{nl}B_{nl}(v)\left(\frac{p}{v}\right)^n P_l(\hat{\mathbf{p}}\cdot\hat{\mathbf{v}}). \tag{11}$$

Introducing this expression in Eq. (10) and using Eq. (8) we obtain

$$\frac{d\sigma}{dP_{R\|}}=4\pi v\,pF(p)\beta_0(v,p) \tag{12}$$

with

$$\beta_0(v,p)=\sum_n B_{n0}(v)\left(\frac{p}{v}\right)^n. \tag{13}$$

Equation (12) provides the RIM distribution near the threshold in terms of the shape parameters $B_{n0}$ describing the ECC peak. It should be pointed out that the coefficients $B_{nl}$ with $l\neq0$ have no influence in the RIM distribution. That is, no information about the ECC asymmetry coefficients $B_{n1}$ can be obtained from RIM measurements near the threshold. Note that in the derivation of Eq. (12) we have kept all the

orders in the small magnitude $p=\sqrt{2v(P_{R\|}-P_{R\|}^{\min})}$. In [11] a similar expression up to the second-order term was obtained.

### III. IONIC PROJECTILES

We can use Eq. (12) to obtain the RIM distribution behavior at the threshold in terms of the $F(p)$ factor,

$$\left.\frac{d\sigma}{dP_{R\|}}\right|_{P_{R\|}^{\min}} = 4\pi v B_{00} \lim_{p\to 0} pF(p). \tag{14}$$

In particular, replacing $F(p)$ by the expression given in Eq. (2) for an ionic projectile of charge $Z_P>0$, we obtain that the longitudinal RIM distribution approaches a finite value given by

$$\left.\frac{d\sigma}{dP_{R\|}}\right|_{P_{R\|}^{\min}} = 8\pi^2 Z_P v B_{00}. \tag{15}$$

On the contrary, for a negatively charged projectile,

$$\frac{d\sigma}{dP_{R\|}} \approx 8\pi^2 Z_P v \ \exp[-2\pi|Z_P|/\sqrt{2v(P_{R\|}-P_{R\|}^{\min})}] \times \beta_0[v, 2v(P_{R\|}-P_{R\|}^{\min})] \tag{16}$$

and the longitudinal RIM distribution approaches zero exponentially.

These results show that the behavior of the longitudinal RIM distribution near the threshold strongly depends on the electron-projectile interaction. For a positively charged projectile, the electronic momentum distribution has a cusp at $p=0$, and $d\sigma/dP_{R\|}$ approaches a finite value for $P_{R\|}\to P_{R\|}^{\min}$. On the contrary, for a negatively charged projectile, the electronic cross section has a dip at $p=0$ and the longitudinal RIM distribution approaches zero exponentially. These results restricted to Coulomb potentials have been obtained in a different way in [11]. In the next section we generalize the study to other types of electron-projectile interactions in the exit channel.

Here we want to illustrate the different behaviors discussed above. In Fig. 2 we show the RIM cross section $d\sigma/dP_{R\|}$ for the $H^+$+He collision at 100 keV (projectile velocity $v=2$ a.u.). We also quote results for antiproton impact at the same energy. The calculation is performed with the continuum-distorted-wave–eikonal-initial state (CDW-EIS) [17] employing the independent electron model described in [18]. For a comparison we show in the same figure results obtained with the first Born approximation.

First, we see clearly that the maxima are located around $P_{R\|}^{s}=|\varepsilon_i|/v\sim 0.45$ a.u., showing the importance of the SE ionization mechanism. However, we note that the location of the proton (antiproton) maximum is shifted towards smaller (larger) values. This shift has been interpreted in [11,19] to arise from postcollision interaction taken into account by CDW-EIS calculations. The soft-electron emission is enhanced in the forward (backward) direction for the proton (antiproton). In the first Born approximation no dependence on the sign of the charge is found and the maximum is located close to $P_{R\|}^{s}$.

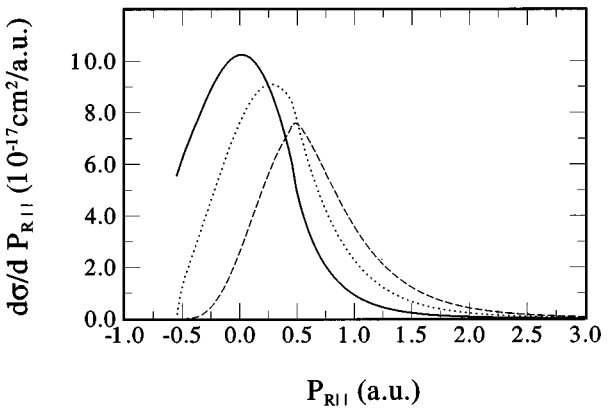


FIG. 2. The longitudinal recoil-ion momentum distribution for single ionization of He by the proton and antiproton at 100 keV ($v=2$ a.u.). Solid (dashed) line: CDW-EIS calculation for proton (antiproton) impact. Dotted line: first Born approximation.

Second, around the threshold $P_{R\|}^{\min}\sim -0.548$ a.u., we can observe how the CDW-EIS results that comply with the final-state interaction theory show for proton impact a finite value at the threshold. For antiproton impact the RIM distribution decreases exponentially as $P_{R\|}$ approaches the threshold. On the other hand, Born results go to zero for either case, but as $\sqrt{2v(P_{R\|}-P_{R\|}^{\min})}$.

### IV. NEUTRAL PROJECTILES

While it can be readily proved that for the case of a pure Coulomb potential of charge $Z_P>0$ the general expression (1) leads to a prominent enhancement of the ionization cross section [as given by the normalization factor (2)], this is not necessarily valid for any arbitrary attractive electron-projectile potential. For instance, for the case of a neutral helium projectile in its ground state, only a very feeble enhancement of the ionization cross section is obtained [20].

In order to clarify the difference between both cases, let us introduce an arbitrary screening of range $R$ in the electron-projectile interaction. It can be shown easily that for $p$ much greater than a quantity of the order of $1/R$, the enhancement factor does not differ from that of a pure Coulomb potential, Eq. (1). However, when $p$ approaches zero, the enhancement factor behaves like [14]

$$F(p)\approx \frac{1}{b^2}\frac{a_0^2}{1+a_0^2p^2}, \tag{17}$$

with $b$ a distance of the order of $R$ for typical atomic potentials and $a_0$ the $s$-wave scattering length for the electron-projectile interaction. The inverse of this scattering length can be shown to be related to the ''distance'' to the origin in the complex $p$ momentum plane of the potential's $s$-wave bound and ''virtual'' states. Whenever the range $R$ of the potential is such that a zero-energy $s$-wave bound state can exist, $1/a_0$ is zero ($a_0\to\infty$), and the enhancement factor diverges as $1/p^2$, an effect known as ''zero-energy resonance'' [13]. In particular, for a pure Coulomb potential, the origin of the complex $p$ plane is an accumulation point of bound states, and the enhancement factor is given by Eq. (2)

all the way down to $p=0$. This description represents the natural generalization for any arbitrary electron-projectile interaction of the original interpretation of the ECC peak as a continuation over the ionization threshold of the cross section for the ''electron capture'' to highly excited states [6].

Generally, an ECC peak with a very broad Lorentzian shape is to be expected for neutral projectiles in their ground states, since their scattering lengths are not particularly large. However, this case does not exhaust all the possibilities. For instance, there are evidences of low-energy bound and virtual states of an electron in the field of excited states of rare-gas and alkali atoms. For instance, the scattering length for the $e+\mathrm{Li}(2\,^2P)$ system is appreciably large. Furthermore, the experimental observations [21–23] of a narrow ECC peak in coincidence with neutral He projectiles have been attributed to the presence of a zero-energy resonance effect produced by a low-lying virtual state in the $e+\mathrm{He}(2\,^1S)$ system [15]. With a scattering length of about $a_0\approx 330$ a.u., a helium projectile in this metastable state can produce an ECC peak that, after integrating over the spectrometer resolution, is much narrower than the usual $1/p$ cusp corresponding to a pure Coulomb interaction.

We are now in the position to describe the behavior at the threshold of the longitudinal recoil-ion momentum cross section for any arbitrary electron-projectile interaction. Replacing $F(p)$ in Eq. (12) by the expression given by Eq. (17) we find that, for $P_{R\|}$ close to $P_{R\|}^{\min}$,

$$\frac{d\sigma}{dP_{R\|}}\approx\frac{4\pi a_0 v}{b^2}\,\frac{a_0 p}{1+a_0^2p^2}\,\beta_0(v,p), \tag{18}$$

with $p=\sqrt{2v(P_{R\|}-P_{R\|}^{\min})}$. It is clear from this expression that $d\sigma/dP_{R\|}$ would approach zero at the threshold for any short-range potential, except at a ''zero-energy resonance'' ($a_0\to\infty$), when the following diverging behavior is to be expected:

$$\frac{d\sigma}{dP_{R\|}}\approx\frac{2\pi}{b^2}\left(\frac{2v}{P_{R\|}-P_{R\|}^{\min}}\right)^{1/2}\beta_0(v,0). \tag{19}$$

In practice, the scattering length $a_0$ is unlikely to be infinite, but—as was previously discussed—it may reach an appreciably large value whenever the electron-projectile system can sustain a weakly bound $s$ state or a low-lying virtual state. In this case the longitudinal RIM cross section would display a sharp peak close to $P_{R\|}^{\min}$.

These different behaviors are displayed in Fig. 3 for the ionization of a He target by the collision of neutral He projectiles in its ground ($1\,^1S$) and metastable ($2\,^1S$ and $2\,^3S$) states at 100 keV/amu ($v=2$ a.u.). The calculation of the corresponding electronic momentum distribution is based on a method described in [15]. The scattering lengths ($a_0$) in Eq. (17) were obtained from calculations by Nesbet [24,25]. For larger values of $p$ Eq. (17) was extended by means of a fitting to the corresponding $F$ factor for a Hulthen-type potential [14].

In Fig. 3, no distinctive structure at the threshold is observed for the $1\,^1S$ state, a result that is consistent with the small value of the corresponding scattering length. On the contrary, the presence of a low-lying virtual state in the electron-projectile system leads to the appearance of an extremely sharp peak very close to the kinematic threshold for the $2\,^1S$ state. The $2\,^3S$ state represents an intermediate situation with a scattering length much smaller, but still large enough to produce a distinctive peak located near $P_{R\|}^{\min}$.

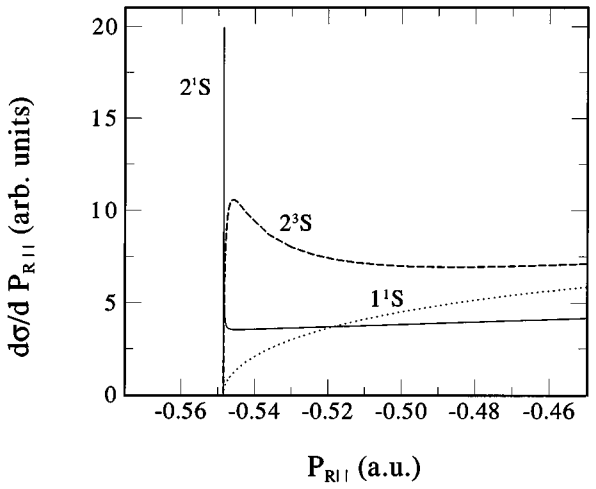


FIG. 3. The longitudinal recoil-ion momentum distribution for single ionization of He by neutral He projectiles in their ground ($1\,^1S$) and metastable ($2\,^1S$ and $2\,^3S$) states at 100 keV/amu ($v=2$ a.u.). All the curves have been arbitrarily normalized to fit in the same linear scale.

## V. FINAL REMARKS

Recently, the presence of an ECC peak in the ionization cross section for the case of neutral H projectiles has been observed experimentally [22]. Whether such an effect can also be explained in terms of the continuity across the ionization threshold remains an open question. The long-range dipolar interaction of the $e+\mathrm{H}(nl)$ system prevents one from making a direct application of the standard theory as presented in this paper. For small values of the relative electron-projectile momentum $p$ the behavior of $F(p)$ in Eq. (1) strongly depends on the way in which the corresponding interaction decreases at infinity. The present description in terms of the scattering length applies only for potentials that decrease faster than $1/r^3$. If the interaction decreases more slowly, singularities at zero energy emerge, as is the case of the dipolar and Coulomb potentials.

The explanation of the ECC process by neutral projectiles in terms of the zero-energy resonance theory represents a direct generalization of the standard understanding of the ECC peak as a continuation over the ionization threshold of the cross section for the electron capture to Rydberg states. Furthermore, the available experimental evidence [21–23] is compatible with this theoretical description. However, some doubts have been cast about its validity [22,26]. In this sense, a longitudinal RIM measurement showing a peak near the threshold will serve as a confirmation of this model, i.e., that the present description of the ECC effect also applies for neutral projectiles.

## ACKNOWLEDGMENTS

This work has been partially supported by the Consejo Nacional de Investigaciones Científicas y Técnicas under PID 3357/92-CONICET. Instituto Balseiro is affiliated with the Universidad Nacional de Cuyo.

[1] M. E. Rudd, Y. Kim, D. Madison, and T. Gay, Rev. Mod. Phys. **64**, 441 (1992).
[2] D. H. Lee, P. Richard, T. J. M. Zouros, J. M. Sanders, J. L. Shinpaugh, and H. Hidmi, Phys. Rev. A **41**, 4816 (1990).
[3] S. Suárez, C. Garibotti, W. Meckbach, and G. Bernardi, Phys. Rev. Lett. **70**, 418 (1992).
[4] G. B. Crooks and M. E. Rudd, Phys. Rev. Lett. **25**, 1599 (1970).
[5] A. Salin, J. Phys. B **2**, 631 (1969).
[6] J. H. Macek, Phys. Rev. A **1**, 235 (1970).
[7] M. W. Lucas and E. Steckelmacher, in *High-Energy Ion-Atom Collisions*, Lecture Notes in Physics Vol. 294 (Springer, Berlin, 1987).
[8] R. G. Pregliasco, C. R. Garibotti, and R. O. Barrachina, J. Phys. B **27**, 1151 (1994).
[9] J. Ullrich, R. Dörner, V. Mergel, O. Jagutzki, L. Spielberger, and H. Schmidt-Böcking, Comments At. Mol. Phys. **30**, 285 (1994).
[10] R. Dörner, V. Mergel, Liu Zhaoyuan, J. Ullrich, L. Spielberger, R. E. Olson, and H. Schmidt-Böcking, J. Phys. B **28**, 435 (1994).
[11] V. D. Rodríguez, Y. D. Wang, and C. D. Lin, Phys. Rev. A **52**, R9 (1995).
[12] J. Gillespie, *Final-State Interactions* (Holden-Day, San Francisco, 1964).
[13] J. R. Taylor, *Scattering Theory* (Wiley, New York, 1972).
[14] R. O. Barrachina and C. R. Garibotti, Lett. Nuovo Cimento **36**, 583 (1983).
[15] R. O. Barrachina, J. Phys. B **23**, 2321 (1990).
[16] W. Meckbach, I. Nemirovsky, and C. R. Garibotti, Phys. Rev. A **24**, 1793 (1981).
[17] D. S. F. Crothers and J. F. McCann, J. Phys. B **16**, 3239 (1983).
[18] P. D. Fainstein, V. H. Ponce, and R. D. Rivarola, J. Phys. B **24**, 3091 (1991).
[19] V. D. Rodríguez, Y. D. Wang, and C. D. Lin, J. Phys. B **28**, L471 (1995).
[20] D. H. Jakubassa-Amundsen, J. Phys. B **22**, 3989 (1989).
[21] L. Sarkadi, J. Pálinkás, A. Kvér, D. Berényi, and T. Vajnai, Phys. Rev. Lett. **62**, 527 (1989).
[22] H. Trabold, G. M. Sigaud, D. Jakubassa-Amundsen, M. Kuzel, O. Heil, and K. O. Groeneveld, Phys. Rev. A **46**, 1270 (1992).
[23] M. Kuzel, L. Sarkadi, J. Pálinkás, P. A. Závodszky, R. Maier, D. Berenyi, and K. O. Groeneveld, Phys. Rev. A **48**, R1745 (1993).
[24] R. K. Nesbet, Phys. Rev. A **20**, 58 (1979).
[25] R. K. Nesbet, J. Phys. B **13**, L193 (1980).
[26] A. Salin, Nucl. Instrum. Methods **86**, 1 (1994).